DESIGN OF A DIE FOR THE COLD COMPACTION CALIBRATION OF POWDERED MATERIALS

Mauricio Barrera[*], *Héctor Sánchez S.*

- ✓ Este artículo forma parte del "Volumen Suplemento" **S1** de *la Revista Latinoamericana de Metalurgia y Materiales* (*RLMM*). Los suplementos de la RLMM son números especiales de la revista dedicados a publicar memorias de congresos.
- ✓ Este suplemento constituye las memorias del congreso "*X Iberoamericano de Metalurgia y Materiales (X IBEROMET)*" celebrado en Cartagena, Colombia, del 13 al 17 de Octubre de 2008.
- ✓ La selección y arbitraje de los trabajos que aparecen en este suplemento fue responsabilidad del Comité Organizador del *X IBEROMET*, quien nombró una comisión *ad-hoc* para este fin (véase editorial de este suplemento).
- ✓ La *RLMM* no sometió estos artículos al proceso regular de arbitraje que utiliza la revista para los números regulares de la misma.
- ✓ Se recomendó el uso de las "Instrucciones para Autores" establecidas por la *RLMM* para la elaboración de los artículos. No obstante, la revisión principal del formato de los artículos que aparecen en este suplemento fue responsabilidad del Comité Organizador del *X IBEROMET*.

Suplemento de la Revista Latinoamericana de Metalurgia y Materiales 2009; **S1** (1): 223-234

DESIGN OF A DIE FOR THE COLD COMPACTION CALIBRATION OF POWDERED MATERIALS

Mauricio Barrera[*]*, Héctor Sánchez S.*

Escuela de Ingeniería de Materiales, Universidad del Valle. Cali, Colombia

E-mail: mbarrera@univalle.edu.co

Trabajos presentados en el X CONGRESO IBEROAMERICANO DE METALURGIA Y MATERIALES IBEROMET
Cartagena de Indias (Colombia), 13 al 17 de Octubre de 2008

Selección de trabajos a cargo de los organizadores del evento

Publicado On-Line el 20-Jul-2009
Disponible en: *www.polimeros.labb.usb.ve/RLMM/home.html*

Abstract

This paper addresses the problem of finding the radial stress within a powder body undergoing plastic deformation by confined compression, motivated by the compaction test for powdered materials. Small deformation, elastoplastic behaviour is assumed, with porosity as the parameter governing the evolution of material properties. An elliptic yield surface is selected, whose aspect ratio approaches zero as full density is neared, so as to recover the Von-Mises criterion of plastic yield in ductile metals. The results were used to track the radial stresses on a notional compaction process, and applied to the design of an instrumented closed die. In addition, the aspect ratio of the yield surface showed an evolution according to the widely used Heckel porosity-pressure function [6], thus extending the interpretation of this model to a more general stress state.

Keywords: *Powder compaction, Powder plasticity, Plasticity model calibration*

Resumen

Este articulo trata el problema de hallar el esfuerzo radial dentro de un espécimen de material en polvo sometido a deformación plástica mediante compresión confinada, motivado por el ensayo de compactación para materiales en aquel estado. Se asume un comportamiento elástico-plástico de pequeñas deformaciones, siendo la porosidad el parámetro que gobierna la evolución de las propiedades del material. Se escoge una superficie elíptica de fluencia plástica, cuya relación de aspecto se aproxima a cero en la medida que el material se acerca a la densificación total. De este modo se recupera el criterio de fluencia plástica de Von-Mises. Los resultados del análisis se usaron para calcular los esfuerzos radiales durante un proceso de compactación propuesto para el caso, y se aplicaron al diseño de un dado de compactación instrumentado. Adicionalmente, la relación de aspecto de la superficie de fluencia mostró una evolución de acuerdo con el modelo porosidad-presión de Heckel [6], extendiendo así la interpretación que se hace de este modelo a una situación de estado de esfuerzo mas general.

Palabras clave: *Compactación de polvos, Plasticidad de polvos, Calibración de modelos de plasticidad*

1 INTRODUCTION

The current context within which manufacturing processes of powder materials are engineered demands a mechanical characterization of the material, considering the multiaxial nature of the stress-strain state. To this purpose the conventional close compaction test [1] must allow for computing the radial stress into the specimen, in addition to the punching -or axial- stress. In particular, a set of strain gauges measuring the hoop strain at the outer surface of the die is laid out to fulfil the requirement [2,3]. Having recourse to thick walled vessel formulae [4] leads to a prompt calculation of the radial stress present in the powder specimen. A crucial point is the determination of an appropriate value for die wall thickness: too thin and it would collapse upon loading of the powder specimen; too thick and hoop strains could not be properly gauged. In the light of this, it is clear that some estimation of radial stress exerted by the powder body, which is undergoing uniaxial confined compression, is to be done in advance. In a first approximation to this problem the analysis of seemingly influential factors, such as die-wall friction and nonuniformities within the specimen thereof -both in axial and radial directions-, is relinquished on

behalf of mathematical tractability. That said, it was decided to turn to a yield surface expression devised for aluminium foams [5], deeming it as makeshift powdered material. The end result is a solution to the problem of uniaxial confined compression of a specimen of increasing relative density, where elastic stresses are stored up until plastic onset, dictated by the mentioned material model, occurs.

In this regards, and to completely define the problem an elastoplastic behaviour assumption comes necessary, whereby elastic behaviour is assumed to be linear and of small strains, and also showing a dependence on the degree of compaction. Elastic computations provide the stress state by means of which plastic yielding is arrived to; the yield function and an assumed associative plastic behaviour provide an update of plastic straining and, hence, of porosity. This is then used to compute new values of elastic constants. The application of this procedure throughout a compaction process permitted to track the evolution of radial stresses, and therefore, the application of thick wall vessel formulae to make a decision in regards of die wall thickness. The compaction die was built and the requirements of structural strength and hoop strain measurement were satisfactorily met. The evolution of the yield surface parameter, called aspect ratio, showed to obey a Heckel-like function [6], thus providing an interpretation of this porosity-pressure model in terms of a more general stress state.

2 THE YIELD FUNCTION

The classic Von-Mises yield function has been modified by several authors intending to represent the observed behaviour in porous materials, where a ductile, metal-like mechanical deformation at full density is attained eventually. One such model is given by Eq.(1):

$$g(\sigma_{ij}) - \sigma_0(k) = 0 \tag{1}$$

The first term represents a function of stress components which is the equivalent stress from Von-Mises theory, including a modification by hydrostatic pressure. The second term stands for yield strength in uniaxial test, whether tension or compression. It shows a dependency on the extent of plastic deformation through an observable parameter k. The function of stresses is given by Eq.(2) [7]:

$$g(\sigma_{ij}) = \frac{\sigma_e^2 + \alpha^2 \sigma_m^2}{\left(1 + \left(\alpha/3\right)^2\right)} \tag{2}$$

It is worth to note how this function is actually a quadratic expression in $\{\sigma_e, \sigma_m\}$ depicting an ellipse on (p,q) plane [9], which has proven adequate in fitting experimental data to results of triaxial test probing of metal foams and some granular materials. It makes part of a more general family of elliptic yield functions of the form [8]:

$$J_2' + \alpha J_1^2 - \delta \sigma_0^2 = 0 \tag{3}$$

posed in terms of stress invariants (J_1, J_2') for stress tensor and stress deviator, and two empirical, material dependent parameters (α, δ).

The stress components shown in the numerator of Eq.(2) stand for the square root of the double contraction of stress deviator –equivalent or effective stress- and one third of the trace of hydrostatic component of stress tensor-mean stress-, as set out in Eq.(4) and Eq.(5):

$$\sigma_e = \left(\frac{3}{2} S_{ij} S_{ij}\right)^{1/2} \tag{4}$$

$$\sigma_m = \frac{1}{3}\sigma_{kk} \tag{5}$$

The parameter α captures the dependency of yield function on hydrostatic stress. At full density, $\alpha = 0$ and the yield function of Von-Mises is recovered. In deriving the yield function, intended to characterize aluminium foams, a material specimen was probed using a triaxial load cell, and the results of Figure 1 were obtained.

It is shown that the yielding of the material is described by an ellipse lying on the (p,q) plane characterized by the ratio α of its semi axes. As this is a material-dependent quantity, the parameter α is a material property called “pressure-sensitivity coefficient”.

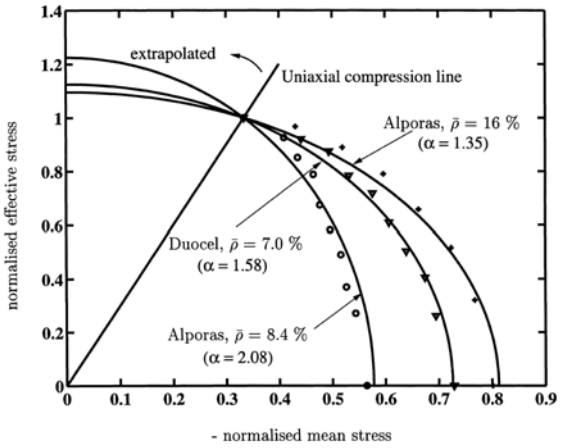

Figure 1. Experimental yield loci for some typical aluminium foams and comparison with elliptic yield surface [7].

As to the coordinate axes in Figure 1, Figure 2 recalls the stress state for a material element undergoing closed die compaction, in terms of punching pressure and radial pressure. Stress components homogeneity throughout the specimen is assumed.

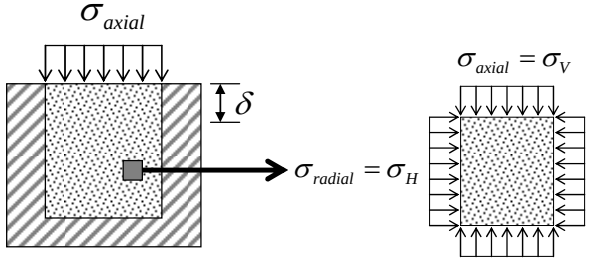

Figure 2. Stress state of a homogeneous specimen undergoing confined compression.

Certainly a relationship between equivalent and mean stress with p and q components of stress may be established, so that Eq.(6) and Eq.(7) hold [9]:

$$\sigma_e = q = \left(\sigma_V - \sigma_H\right) \tag{6}$$

$$\sigma_m = p = \frac{\sigma_V + 2\sigma_H}{3} \tag{7}$$

3 CONFINED COMPRESSION OF A METAL FOAM

The aim is to know what the radial pressure is that a specimen of metal foam, undergoing closed die compaction, would exert. This material is considered, in the approximation presented here, as appropriately taking the place of a metal powder body. Replacing Eq.(2) in Eq.(1) and from the considerations leading to Eq.(6) and Eq.(7) it is possible to state Eq.(8)

$$\sigma_0\left(k(\rho)\right) = \frac{1}{\left(1+\left(\alpha/3\right)^2\right)}\left[\begin{matrix}\sigma_e^2\left(\sigma_V,\sigma_H\right)+\\ \alpha^2\sigma_m^2\left(\sigma_V,\sigma_H\right)\end{matrix}\right] \tag{8}$$

The observable material parameter k to the left hand side of the equation has been made dependent on density, i.e. density is the quantity used to track the evolution of plastic deformation of the material.

As the punching stress, represented by σ_V, is the experimental input in a closed die compaction test, and also as this happens to be the yield strength of the tested material throughout compaction, the aim is to solve Eq.(8) for it. Nonetheless an issue is yet to be addressed, namely, the way the radial stress exerted against the die wall is generated. At this point it is assumed that elastic behaviour is responsible for storing that energy which carries over to exerted radial pressure. Linear elastic, small strains behaviour is assumed at this point. This in conjunction with presumed homogeneity within the specimen permits to state the generalized Hooke's law to an axisymmetric element, as shown in Figure 3 and rearranged in Eq.(9).

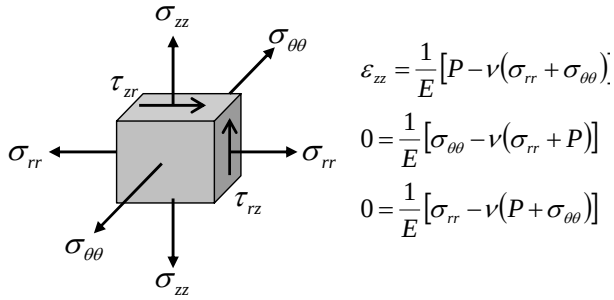

Figure 3. Axisymmetric stress state and generalized Hooke law to the case.

$$\begin{bmatrix} B & -A & 0 \\ -A & B & 0 \\ -A & -A & 1 \end{bmatrix}\begin{Bmatrix}\sigma_{\theta\theta}\\ \sigma_{rr}\\ \varepsilon_{zz}\end{Bmatrix} = P\begin{Bmatrix}A\\ A\\ B\end{Bmatrix} \tag{9}$$

In Eq.(9) $A \equiv \nu E^{-1}$ and $B \equiv E^{-1}$. The linear dependence of the first two equations in Eq.(9)

shows that radial and transverse stress components equal each other. This is why a single component is given to them in the context of stress states on (p,q) plane, where axisymmetric stress states are assumed (i.e. $\sigma_{rr} = \sigma_{\theta\theta} = \sigma_H$).

Solving for radial stress yields Eq.(10):

$$\sigma_{rr} = P\left(\frac{A}{B-A}\right) = PK \tag{10}$$

The last term to the right is just shorthand for upcoming derivations. This result may now be replaced back into Eq.(8) and solved for punching stress $\sigma_{zz} = \sigma_V = P$, resulting in Eq.(11) below:

$$P = \sigma_0(\rho)\left(\frac{\left(1+\alpha^2/9\right)}{(1-K)^2+\alpha^2/9\,(1+2K)^2}\right)^{1/2} \tag{11}$$

Eq.(11) can be thought of as the yield strength of the material under closed die compaction. It is worth to recall that a yielding point is arrived to by means of storing energy by previous deformation, and it is the elastic regime of the material where this storage takes place.

So, here lies the central assumption to the derivation just conducted: the radial stress component is taken to be an immediate consequence of the confined compaction carried out by the punching stress and a presumed linear elastic behaviour of the material. It is this link between stress components, stemming from the axisymmetric, confined compression mechanical condition what allowed for the expression in Eq.(11) to be gained.

4 EVOLUTION EQUATIONS: YIELD SURFACE

It is left now to specify the way in which the yield surface aspect ratio α , yield strength under uniaxial loading $\sigma_0(k(\rho))$ and elastic properties K depend upon a measure of plastic deformation. Relative density will serve the purpose, in a first approximation since, in so doing, the second invariant of the strain tensor is being neglected as a measure of deformation. Then $\alpha(\rho)$ and $\{E(\rho),\nu(\rho)\}$ shall be sought in the sequel.

As to the yield surface aspect ratio, it is necessary to recall that Eq.(2) was originally intended to represent the yield behaviour of a metal foam. Such a material is not purported to deform plastically by reducing its porosity up until attaining full density, unlike metal powders during compaction. The yield function in Eq.(2), within the context of metal foams, is said to evolve in a self-similar manner, so that the aspect ratio α is virtually a constant throughout the plastic deformation process. The hardening rules to that particular case are derived from application of Prandtl-Reuss plastic flow rule and definition of a work conjugate stress-strain pair, in such a way that the tangent modulus from readily conducted tests, such as hydrostatic and uniaxial loading, may be used to characterize the way a material hardens plastically.

To make the case for powder compaction one could resort to some results of triaxial probing over metal powder specimens showing that, at least during the first stages of compaction, the yield surface is appropriately represented by an ellipse. Now, as the powder is intended to attain full density, aspect ratio must be made variable with relative density. So, an evolution like that set out in Figure 4 is pursued.

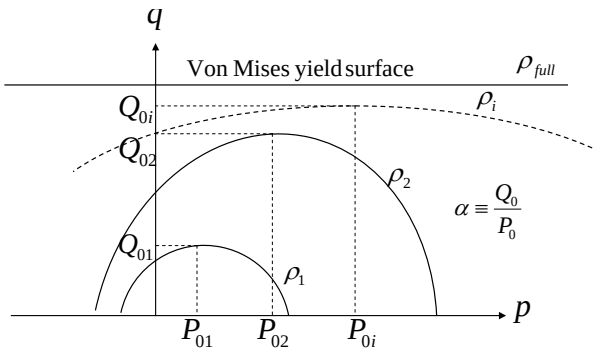

Figure 4. Intended yield surface and its evolution with relative density.

A hint to the functional form of $\alpha(\rho)$ is provided by the measured evolution of the Cam-Clay yield function as applied to some metal powders of industrial interest. The evolution of the ellipses, characterized by their semi axis lengths (P_0, Q_0) is described by the function shown in Eq.(12) [2].

$$Q_0 = Q_{\max}\tanh\left(\frac{K_1 P_0}{Q_{\max}}\right) \tag{12}$$

It is clearly a non trivial task to solve analytically for $\alpha = Q_0 P_0^{-1}$. Yet, from the same reference, P_0 is taken as the yield surface parameter uniquely

defining yield surface shape and also uniquely depending on relative density. A particular form of this dependency was found to be given by Eq.(13)

$$P_0 = K_2\left(\ln\left(1-\frac{\rho-\rho_0}{\rho-\rho_{full}}\right)\right)^{K_3} \qquad (13)$$

In this equation $(\rho, \rho_0, \rho_{\max})$ stand for current density, apparent density and maximum (theoretical) density of the powdered material, respectively.

Equations Eq(12) and Eq.(13) turned out to be satisfactory fitting functions and are not prescriptive, i.e. experimental data from other materials may quite well be fitted by some other functions. Nonetheless, it is always preferred to use functions which are somehow related with powder compaction models, particularly in regards of Eq.(13). Being this the case, a physical meaning of the fitting parameters is gained. In this sense it is worth to mention that compaction models relating P_0 with ρ, such as that of Heckel [6], are widely employed for this specific purpose.

The case was made for an iron alloy powder, which bore a yield strength of 170MPa ($Q_{\max}$) after compaction. Fitting parameters were 1.5, 21.903 and 1.3527 for $\{K_1, K_2, K_3\}$ respectively [2]. Tabulating data from Eq.(12) and Eq.(13) provides a mean to track the progress $\alpha(\rho)$ sought for.

Table 1 displays the results of a compaction process of up to 87.5% of full density for an iron powder (density 7.8Kg/m^3), which is what in practice is reached to such a material.

Table 1. Data from a compaction process, iron powder.

Current density (Kg/m^3)	*P_0 (MPa)*	*Q_0 (MPa)*	*Aspect Ratio α*
2.808	0.000	0.000	-
5.803	19.460	28.907	1.485
6.802	41.694	59.864	1.436
7.301	67.682	90.958	1.344

Apparent density (Kg/m^3): 2.808; Theoretical density (Kg/m^3): 7.8; $Q_{\max}$ (MPa): 170 [2]

It can be seen that the aspect ratio changes are negligible and that a Von-Mises yield surface might not be recovered this way. However, assuming that from this compaction state up to full density there are not changes in material phenomena underlying fitting parameters $\{K_1, K_2, K_3\}$, one may actually approach the theoretical density (7.8 Kgm^{-3}). Results are set out in Table 2 below.

Table 2. Yield surface aspect ratio on using Eq.(13) for extrapolation.

Current density (Kg/m^3)	*P_0 (MPa)*	*Q_0 (MPa)*	*Aspect Ratio α*
7.650	119.603	133.257	1.114
7.794	292.428	168.060	0.575
7.797	337.976	169.129	0.500
7.799	429.565	169.827	0.395

It can be seen that the yield surface actually tends to approach Von-Mises yield surface in a noticeable manner only as density is within 2% before theoretical density. Then, one may take these just tabulated results to perform a curve fitting leading to an evolution equation $\alpha(\rho)$. The following variable modification, Eq.(14), is enforced so that curve fitting results do not resort to an unwieldy set of empirical constants, which would make a physical interpretation nearly impossible.

$$Ln(\alpha) = Ln\left(\frac{1}{1-\dfrac{\rho}{\rho_{full}}}\right) \qquad (14)$$

Plotting this equation leads to Figure 5 below.

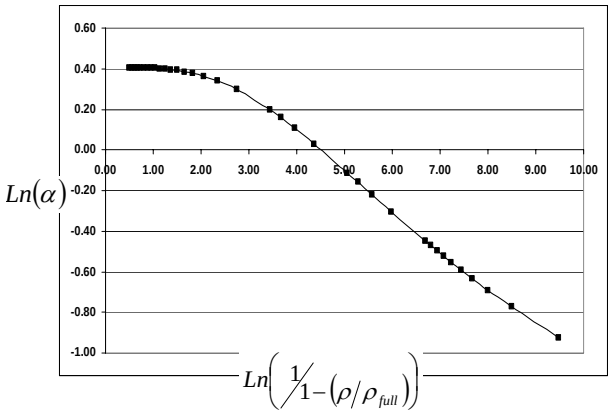

Figure 5. Evolution of yield surface aspect ratio with a logarithmic function of relative density.

From the value 2.00 (corresponding to a relative density of about 87%) for the abscissa towards the right, a straight line would provide a satisfactory fitting, indicating an exponential-like relationship between the plotted parameters. So, the dependence $\alpha(\rho)$ could be split into two ranges:

From apparent density to 87% full density: aspect ratio is almost a constant, with a value of $\alpha \approx 1.5$. Yield surface evolution is self similar, and provided a triaxial probing over a body of metal powder confirms this self similarity, metal foam yield flow behaviour might be thought of as a fairly good imitation of that of metal powder. This does not mean that at a micro-scale level the same plastic flow mechanisms come upon in metal foams and metal powders.

From relative density 87.5% up until full, theoretical density: aspect ratio varies in order to recover the Von-Mises yield surface as the material gains full density. It is by virtue of Eq.(13) that self similarity breakdown takes place. As full density is neared P_0 tends to infinity and Q_0 tends to $Q_{\max}$. As seen, this could only be explored by means of curve fitting functions, for the practical limits of powder compaction processes prevent compaction densities close to 100% from being achieved.

Cold compaction of a typical iron powder shows, in addition, that most of the compaction takes place at relative densities above 80%, and indicates a practical limit of about 7.2 Kg/m^3 [10].

For relative densities of 80% and above, Figure 6 shows a point selection fitting a straight line. The fitting function is given by Eq.(15) thereafter.

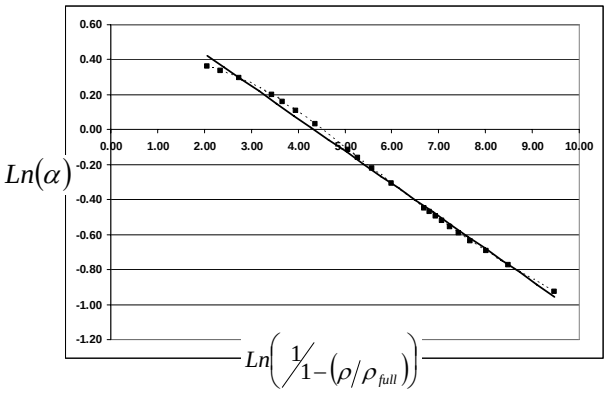

Figure 6. Linear fitting to compaction data at high relative densities (>80%)

$$\ln(\alpha) = -0.177 \ln\left(\frac{1}{1-(\rho/\rho_{full})}\right) + 0.378 \qquad (15)$$

Eq.(15) is actually a linearization of Eq.(16), which is the sought evolution equation $\alpha(\rho)$.

$$\alpha(\rho) = 1.459\left(\frac{1}{1-(\rho/\rho_{full})}\right)^{-0.177} \qquad (16)$$

Now, the way in which uniaxial yield strength σ_0 depends on density is also necessary to perform computations based on the formulations above, and in particular, to make use of Eq.(11). From metal foam studies, whose specimens are appropriately subject to uniaxial loading tests, the following empirical scaling formula is brought in [5,11], Eq.(17).

$$\sigma_0 = \sigma_0(\rho) = 0.3\sigma_y\left(\frac{\rho}{\rho_{full}}\right)^2 \qquad (17)$$

Factors 0.3 and 2 come from curve-fitting exercises, and are used to sort out different metal foam microstructures; σ_y stands for the yield strength of the full dense material. Yet, it is noted that this scaling law embodies the fact that metal foams are not intended to deform plastically so as to attain full density: for a relative density of 1.0 yield strength would only be one third that of the full dense material. On accounts of that a much simpler expression, yet more abiding to experimental observations, is put forward to use, Eq.(18):

$$\sigma_0 = \sigma_y\left(\frac{\rho}{\rho_{full}}\right) \qquad (18)$$

Microstructure issues of apparent relevance to metal powders are spared from analysis. Worth to mention is that a full dense material obtained from powder compaction may show plastic deformation mechanisms different from those of wrought materials: contact points between particles are usually tainted with impurities which might quite well influence dislocation slip mechanisms.

5 SCALING EQUATIONS FOR ELASTIC PARAMETERS

In a like manner to uniaxial yield strength dependence on density, scaling of elastic parameters is also brought from rather empirical, curve fitting

exercises which, however, have proven useful in leading to handy, yet accurate models of material behaviour. So, elastic modulus may be related to density as shown in Eq.(19) [5,11]:

$$E = E(\rho) = 0.3E_{full}\left(\rho/\rho_{full}\right)^2 \qquad (19)$$

Once again, 0.3 and 2 account for microstructure features of some specific metal foam; also, E_{full} stands for Young modulus to the full dense material. Poisson ratio has been said to be 0.3, typical of many full dense structural metals, and not bearing a noticeable dependence on density. Nonetheless, an empirical study performed over porous structural metals obtained by sintering of porous compacts provided the following relationship, employed herein [11]:

$$\nu = \nu(\rho) = 0.068\exp\left(1.37\left(\rho/\rho_{full}\right)\right) \qquad (20)$$

From the discussion following Eq.(11) radial stress computation comes after two steps: First, define a set of relative densities spanning over the range of densities. $\left\{\rho_0/\rho_{full}, \rho_1/\rho_{full}, \rho_2/\rho_{full} ..., 1\right\}$; Second, compute the value of material properties (elastic and plastic) from evolution equations provided. To each one of the set of relative densities, compute the punching pressure P from Eq.(11). This punching pressure is at equilibrium with elastic deformation of a porous body of the selected relative density, and imposes a plastic deformation corresponding to that relative density as well. Finally, radial stress are computed following Eq.(10).

From elaborated material data and evolution laws, corresponding to a quite general class of an iron alloy porous body, computations are shown in Table 3 (the following values were used: $E_{full} = 200GPa; \sigma_y = 200MPa$).

6 RADIAL STRESS COMPUTATIONS

Table 3. Material data from compaction of an iron alloy powder [UWS, 2007], and resulting radial stresses.

Relative density	*E*	*ν*	*α*	σ_y	*P (MPa)*	*PFullDense (MPa)*	*VonMises Fraction*	*Radial Stress (MPa)*
0.448	1.20E+10	0.13	1.500	8.95E+07	93.41	233.52	0.40	13.41
0.675	2.73E+10	0.17	1.500	1.35E+08	142.07	252.18	0.56	29.40
0.870	4.54E+10	0.22	1.017	1.74E+08	206.46	281.12	0.73	59.58
1.000	6.00E+10	0.27	0.003	2.00E+08	315.15	315.15	1.00	115.15

In addition to the sought figures for radial stress, data labelled as "P Full Dense" and "Von Mises Fraction" is provided too. The former refers to the punching load that should be applied if a full dense material of corresponding yield strength were to be taken to its plastic yielding onset. Comparison with the actual punching pressure P required to incur plastic yield in the porous material provides a sense of how porosity makes for easier yielding under applied load, and also the way a full dense, Von-Mises behaviour is recovered as, indeed, full density is attained and yield surface aspect ratio α reduces to zero. The latter provides a figure of this recovering process, and is plotted in Figure 7 below.

Point 1 in Figure 7 corresponds to the last value where a constant aspect ratio α of 1.5 is employed. Point 2 corresponds to a relative density of 0.87, and from this point on the evolution equation Eq.(16) is employed. There is a noticeable change when moving on between these ranges, due to the fact of using models which try to represent data in Table 1 and Table 2. Also the sharp transition from point 3 to point 4 is a reflection of how the material model rushes to recover Von Mises plasticity only at relative densities close to unity.

Radial stress data are used to estimate die wall thickness in accordance with the requirements laid down in the Introduction to this paper. This and other details of the closed die design are exposed next on.

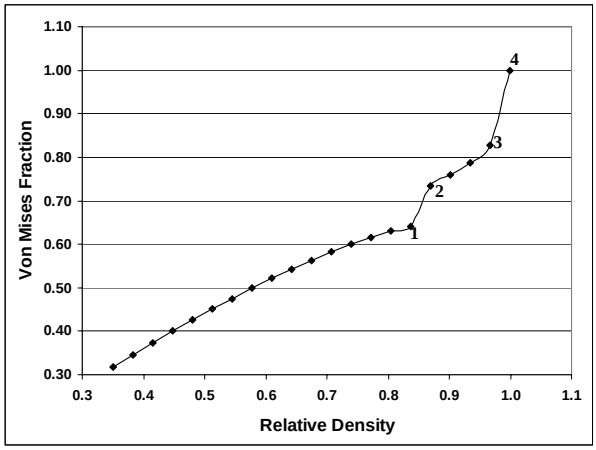

Figure 7. Approximation to Von Mises-like behaviour at relative densities close to theoretical.

7 CLOSED DIE DESIGN

Common constitutive equations for mechanical behaviour of granular bodies imply a joint evolution of axial stress, radial stress and porosity within the specimen, which must be traced out so that the resulting plots convey the desired material parameters. This is actually the problem whose solution is sought when designing a parameter identification rig. It will be henceforth regarded as Measuring Instrument, or just MI.

The MI aimed at in this study is as set out below, Figure 8.

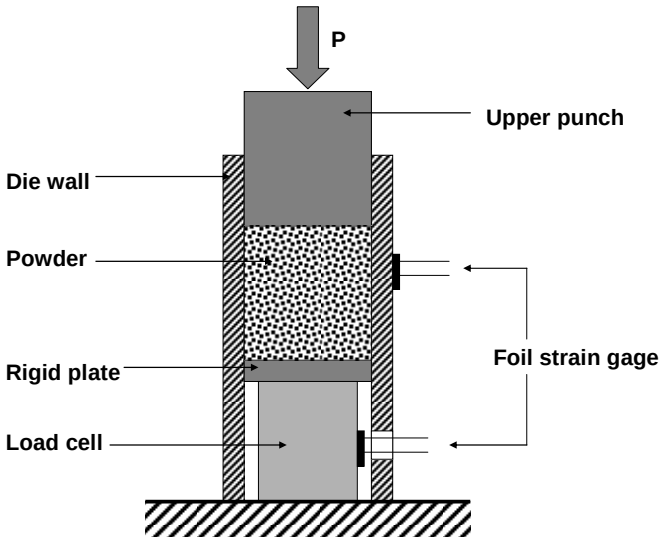

Figure 8. Scheme of the instrumented closed die.

The upper punch load conveys an axial stress σ_{axial} to the powder body. The die wall is rigid so that it is a kinematic constraint and a radial stress σ_{radial} is developed. These two stresses allow for computing stress invariants p and q (or their related quantities σ_e Eq.(4) and σ_m, Eq.(5)). Upper punch displacement data permits volumetric strain computation in turn.

1.1 Specimen size

First considerations come from specimen height to cross section diameter relationship H/D: the larger H/D, the more inhomogeneous and more expensive the specimen. However, an H/D too small would give a total punch displacement small enough so that quite few experimental points could be taken without interfering with punch travel device accuracy figure. In addition, failure tests to the powder body at different relative densities (e.g. unconfined compression test, Brazilian disc test [12]) might impose a lower bound on H/D ratio as well. This all adds to the need of making room for the foil strain gage to capture actual data from powder compaction. With a bore diameter of 12.5mm as starting point, and a maximum H/D of four, pressure versus fractional porosity data from references [11] were used to compute the required punch displacements to seven figures of fill level heights (from 30 mm to 116 mm), as set out in Table 4.

Punch travel for different relative densities and different fill level heights has been computed. As fill level increases, so does punch travel. For a 30mm figure, punch travel roughly ranges from 5mm to 10mm. Now it depends on the punch displacement measuring device the decision whether this range is large enough to take about 10 experimental points without concern as to the measuring instrument accuracy. For the present study a loose powder cylindrical specimen of 30mm height and 12.5mm diameter was deemed appropriate. It is worth to recall, however, that obtaining compacts for failure tests at different, intermediate densities shall require fill level heights of at least 30mm.

1.2 Radial stress, hoop strain

σ_{radial} is computed indirectly from the hoop (or tangential) strain on die wall's outer surface ε_θ. Here the relationship $\varepsilon_\theta = f(\sigma_{radial})$ is called "transduction equation", and is obtained as follows, according to Figure 9.

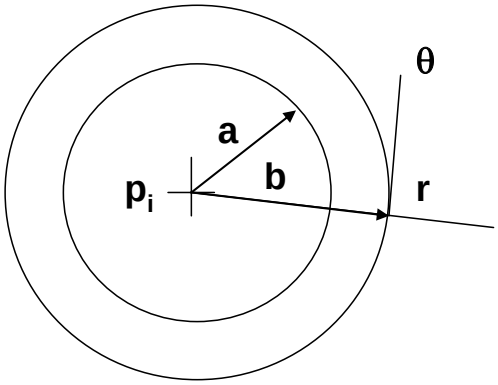

Figure 9. Geometric characterization of the closed die cross section, for design purposes.

Considering the die wall as a thick walled cylinder, hoop strain for plane strain condition is given by [13]:

$$\varepsilon_\theta = \frac{1}{E}\left[\sigma_\theta - \nu\left(\sigma_r + \sigma_z\right)\right] \tag{21}$$

$$\sigma_z = \nu\left(\sigma_r + \sigma_\theta\right) \tag{22}$$

At $r = b$, where hoop strain is to be measured, there is a free surface, so $\sigma_r = 0$ and one is left with:

$$\varepsilon_\theta = \frac{1}{E}\left[\sigma_\theta\left(1-\nu^2\right)\right] \tag{23}$$

It may be found in reference [13] that for a non rotating, thick walled cylinder:

$$\sigma_\theta = \frac{a^2 p_i}{b^2 - a^2}\left(1 + \frac{b^2}{r^2}\right) \tag{24}$$

Where p_i stands for internal pressure. In the present case this is precisely σ_{radial} exerted by the loaded specimen. Enforcing $r = b$ and substituting back gives:

$$\varepsilon_\theta = f\left(\sigma_{radial}\right) = \left[\frac{2a^2\left(1-\nu^2\right)}{E\left(b^2 - a^2\right)}\right]\sigma_{radial} \tag{25}$$

Table 4. Necessary punch displacements (mm) to achieve densities near to theoretical, for typical metal powders [German, 1994], given several figures of fill level heights.

Material	*1 -(Relative Density)*	*P(Mpa)*	*30*	*45*	*60*	*75*	*90*	*100*	*116*
Bronze (Spherical)1	0.35	0	0.00	0.00	0.00	0.00	0.00	0.00	0.00
	0.04	1000	9.69	14.53	19.38	24.22	29.06	32.29	37.46
Copper (Spherical)2	0.22	100	0.00	0.00	0.00	0.00	0.00	0.00	0.00
	0.054	520	5.26	7.90	10.53	13.16	15.79	17.55	20.36
Iron (Sponge)2	0.28	150	0.00	0.00	0.00	0.00	0.00	0.00	0.00
	0.12	610	5.45	8.18	10.91	13.64	16.36	18.18	21.09
Stainless steel 2	0.4	150	0.00	0.00	0.00	0.00	0.00	0.00	0.00
	0.16	770	8.57	12.86	17.14	21.43	25.71	28.57	33.14

Required punch displacements equal to zero indicate the onset of load application.

And this is the "transduction equation". Radial stress within the specimen can be taken from Table 3. The resulting hoop microstrains for a 10mm die wall thicknesses $(b-a)$ are given in Table 5. Die wall is to be made of tool steel ($E = 200GPa; \nu = 0.3$).

Table 5. Radial stresses and hoop microstrains for a compaction process.

Radial Stress (Mpa)	*Hoop microstrain*
13.41	21.18
32.55	51.42
66.88	105.66
115.15	181.92

The hoop strains shown in Table 5 can be readily measured by currently available foil strain gages, so a die wall thickness of 10mm was selected to build the compaction die.

1.3 Axial stress, assemblage

The load cell beneath the powder specimen provides data to asses a correction to upper punch pressure with due to die wall-powder friction during compaction. Both upper punch and a bottom plate are rigid, whereas the load cell body is made of a linear elastic material whose strain upon load application is high enough to be captured by means of an attached foil strain gage. References [3] show that after total loading, load cell force is of up to 90% that from upper punch. This provides a clue on design features.

From data in Table 4, upper punch pressure ranges from about 100MPa the lowest to 1000MPa the highest. This means a 90-900MPa range on the load cell. At this point a decision was made in regards of lower punch cross sectional area: the arrangement of Figure 10 shows, in addition to the assemblage description and picture, that this area is the same as that of the specimen. This ensures that the lower punch, which acts as a load cell, does not collapse at high compaction pressures, and also that punching force line and bottom punch axis are adequately aligned.

Metal plates onto the top punch and beneath the bottom one were added to prevent the pressing machine plates from denting.

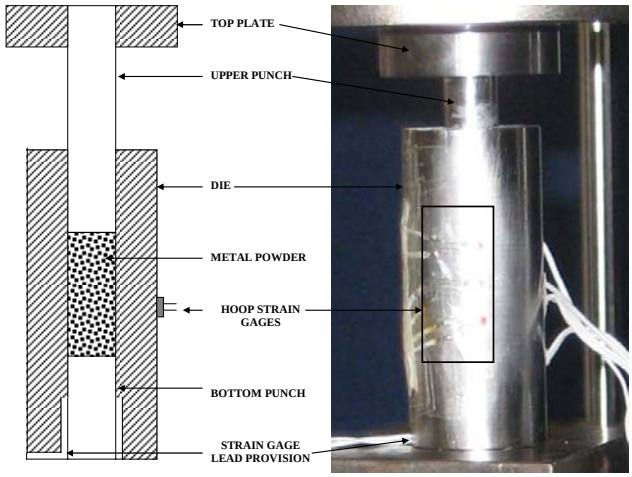

Figure 10. Instrumented closed die.

Using a tool steel bottom punch cell would convey a 5000με strain under 1000MPa of pressure just over the surface in contact with the powder. This hints a limit in top punch applied stress should be considered. Specifically, and in order to meet reported punching pressures to attain high compaction density in a wide variety of metal powders of industrial interest, upper punch stress is bounded to 800MPa, So that, at worst, a 3600με strain (considering an up to 10% loss of punch pressure on accounts of die wall-powder friction) is obtained. A typical foil strain gage holds its measuring features up until 4000με.

1.4 Volumetric strain

Upper punch displacement δ is directly related to the volume change of the specimen, and a strain can be calculated thereof, Figure 11.

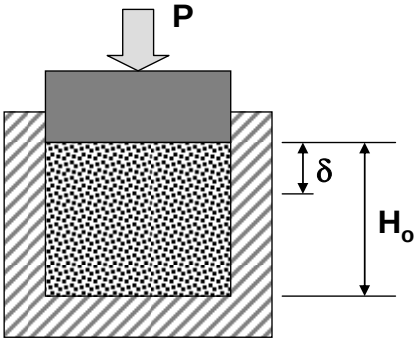

Figure 11. Data for volumetric strain calculation

Here H_o is the initial, fill level height. From data in Table 4 δ may be of up to 10mm for H_o of 30mm (see discussion on specimen size determination). This gives a volumetric strain $\varepsilon_v = \Delta V / V$ of about 33%. Thus, a logarithmic measure of strain must be considered, yielding:

$$d\varepsilon_v = \frac{dV}{V} \Rightarrow \varepsilon_v = \ln\left(\frac{V_f}{V_o}\right) = \ln\left(\frac{H_o - \delta}{H_o}\right) \qquad (26)$$

Relative density is frequently used to characterize the material evolution throughout compaction, and is computed as shown by Eq.(27).

$$R_D(\delta) = \frac{4m}{\pi D^2 \rho_{full}(H_0 - \delta)} \qquad (27)$$

Bring m the mass of the specimen.

1.5 Design tolerances

References from powder compaction tooling designers [14] provided design tolerances and material specifications (AISI D2 cold work tool steel; hardness greater than of equal to 62HRC on contact surfaces), which where also used to check that elastic deformations under applied loads were within design limits, and in particular, that radial straining of the punches inside the die did not interfere with the punching stress intended to deform the powder body. Figure 12 shows construction details.

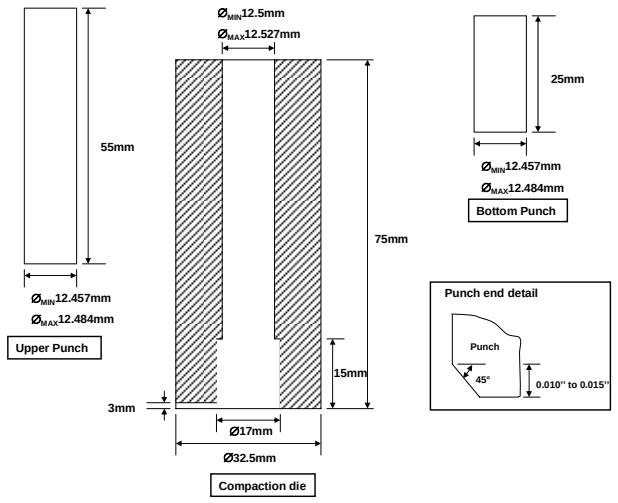

Figure 12. Construction details of the closed die and punches.

8 CONCLUDING REMARKS

In regards of the material model employed to solve the closed die compaction problem in order to get a figure of radial stress exerted by the material against the die wall, it is worth remarking that it was a conjunction of assumed linear elastic, small strain behaviour, with a porosity dependent yield criterion and a Von Mises plasticity recovering at high relative densities. The validity of this model was assumed on the reported elliptic shape of the yield surface for metal foams, which were deemed an appropriate example of porous bodies at low densities; and that at full densities the material was a ductile one, so that Von Mises yield surface proves right.

The model was successfully solved for the close die compaction case, and in particular, a maximum value of radial stresses was the expected outcome. It represents advancement in that, previously, trial and test prototype building was the manner of finding out radial stresses at the design stage of instrumented dies.

Concerning the instrumented die construction three hoop strain gages were attached to the outer surface of the die. They are aimed at capturing a radial stress variation along the specimen length on accounts of sliding die wall friction. The setup was used to study this problematic [15], whose results are expected to be published in the near future

Accuracy and precision of measurements can be computed from basic standard data from strain gages along with computations from Eq.(25) and data in Figure 12 ($E = 200GPa; \nu = 0.3$ are taken from general references so their scatter is considered zero); and also from pressing machine load cell accuracy and cross section area of top punch, bearing in mind its tolerances from Figure 12 as well. Further refinements are aimed at specifying uncertainty figures to alignment/misalignment of hoop strains when attached onto the die surface.

9 REFERENCES

[1] Standard ASTM B331-85: Compressibility of Metal Powders in Uniaxial Compaction, Vol. 02.05American Society for Testing and Materials, 1990.

[2] U.W.S.(University of Wales Swansea), Civil and Computational Engineering Centre. MERLIN

powder compaction software: user's manual. 2007.

[3] Zavaliangos, A., Cunningham, J., Sinka, I.C. J. of Pharm. Sci. 2004; 93 (8).

[4] Budynas, R. Advanced Strength and Applied Stress Analysis. McGraw-Hill, 1999.

[5] Ashby, M.F. et al. Metal Foams: a Design Guide. Butterworht-Heinemann, 2000.

[6] *Heckel, R.W.* Trans. Metall. Soc. AIME. 1961; (221): 671.

[7] *Deshpande, V.S., Fleck, N.A. J. Mech. Phys. Solids. 1999; (48): 1253-1283.*

[8] Green, R.J. International Journal of Mechanical Sciences. 1972; (14): 215-224.

[9] Terzaghi, K. Soil Mechanics in Engineering Practice. 2nd Edition. John Wiley & Sons, 1967.

[10] Hoganas. Iron Powder Handbook. 1957; 1.

[11] German, R. *Powder Metallurgy Science*, 2nd Edition. MPIF, Princeton, NJ., 1994.

[12] Stagg, R.G. Rock Mechanics in Engineering Practice. John Wiley & Sons, 1968.

[13] Timoshenko, S. Theory of Elasticity, 3rd Edition. McGraw-Hill, 1970.

[14] Kunkel, R. Manufacturing Engineering & Management. 1970; 240-244.

[15] Barrera, M. Construction of a True Compaction Curve: Critical Review of the Closed Die Compaction Test for Powdered Materials. PhD Thesis Cali (Colombia), Materials Engineering School, Universidad del Valle, 2008.